Electrocatalysis

International Edition: DOI: 10.1002/anie.201800705
German Edition: DOI: 10.1002/ange.201800705

A Highly Active N-Heterocyclic Carbene Manganese(I) Complex for Selective Electrocatalytic CO_2 Reduction to CO

Federico Franco, Mara F. Pinto, Beatriz Royo, and Julio Lloret-Fillol**

Abstract: *We report here the first purely organometallic fac-[$Mn^I(CO)_3$(bis-^{Me}NHC)Br] complex with unprecedented activity for the selective electrocatalytic reduction of CO_2 to CO, exceeding 100 turnovers with excellent faradaic yields ($\eta_{CO} \approx 95\,\%$) in anhydrous CH_3CN. Under the same conditions, a maximum turnover frequency (TOF_{max}) of 2100 s^{-1} was measured by cyclic voltammetry, which clearly exceeds the values reported for other manganese-based catalysts. Moreover, the addition of water leads to the highest TOF_{max} value (ca. 320 000 s^{-1}) ever reported for a manganese-based catalyst. A Mn^I tetracarbonyl intermediate was detected under catalytic conditions for the first time.*

The large-scale production of value-added chemicals and fuels from renewable energy and CO_2 as a feedstock would contribute to increasing the sustainability of our society.[1] Despite the increasing number of homogeneous catalysts based on earth-abundant transition metals that are able to reduce CO_2,[2] further catalyst development is needed not only to achieve high catalytic rates, better selectivity for a specific product, and long durability, but also to better understand the operative mechanisms for CO_2 reduction.

Among the different families of molecular catalysts reported to be active for selective electrochemical $2e^-$ reductions of CO_2 to CO, metal-based porphyrins and polypyridine complexes show promising results in terms of their activity and stability.[1–3] In particular, Mn *fac*-tricarbonyl derivatives with polypyridyl moieties are able to catalyse the production of CO from CO_2 with high faradaic efficiencies (η_{CO}) in the presence of Brønsted or Lewis acids (Figure 1).[4] However, their further improvement is mainly limited to the functionalization of the bipyridyl[4,5] or pyridyl[6] ligands, whereas reported examples of catalysts with non-pyridyl diimine units are still rare and usually inefficient.[7]

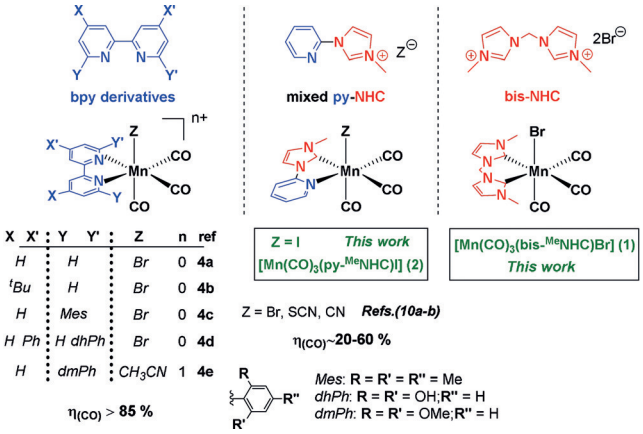

Figure 1. Selected Mn^I catalysts for electrocatalytic CO_2-to-CO reduction with N^N and N^C ligands reported in the literature and complexes **1** and **2**.

In this regard, N-heterocyclic carbenes (NHCs) are attractive for catalysis[8] owing to their strong σ-donor and weak π-acceptor properties, which lead to unique stability. However, several NHC-based molecular complexes show low efficiency in CO_2 reduction and low catalyst stability,[9] such as tricarbonyl pyridyl-NHC Mn^I complexes (Figure 1).[10]

Herein, we explore the electrocatalytic CO_2 reduction properties of the new manganese complex [$Mn(CO)_3$(bis-^{Me}NHC)Br] (**1**), bearing the readily available bidentate methylene bis(*N*-methylimidazolium) ligand bis-^{Me}NHC (Figure 1). For comparative reasons, we also evaluated the catalytic properties of the [$Mn(CO)_3$(py-^{Me}NHC)I] complex (py-^{Me}NHC = *N*-methyl-*N*′-2-pyridylimidazolium; **2**) under the same reaction conditions.

Complex **1** was prepared from a reaction of the bis-^{Me}NHC with [$MnBr(CO)_5$] in the presence of KO^{t}Bu and unambiguously characterized (see the Supporting Information, Figures S1–S7). According to the IR and ^{13}C NMR spectra, the Mn^I centre is facially coordinated by three CO ligands and metalated by the bis-^{Me}NHC ligand, as indicated by the characteristic ^{13}C NMR signal for the carbene carbon atom at $\delta = 189.2$ ppm. Single-crystal X-ray diffraction analysis confirmed the octahedral structure of **1** (Figure 2), with $Mn–C_{(carbene)}$ bond lengths of 2.041–2.043(2) Å, in accordance with previously reported complexes.[8c] Complex **2** was prepared following a reported procedure.[10a]

[*] Dr. F. Franco, Prof. Dr. J. Lloret-Fillol
Institute of Chemical Research of Catalonia (ICIQ)
The Barcelona Institute of Science and Technology
Avinguda Països Catalans 16, 43007 Tarragona (Spain)
E-mail: jlloret@iciq.es
M. F. Pinto, Prof. Dr. B. Royo
Instituto de Tecnologia Química e Biológica António Xavier (ITQB)
Nova University of Lisbon
Av. da República, 2780-157 Oeiras (Portugal)
E-mail: broyo@itqb.unl.pt
Prof. Dr. J. Lloret-Fillol
Catalan Institution for Research and Advanced Studies (ICREA)
Passeig Lluïs Companys, 23, 08010 Barcelona (Spain)
Supporting information and the ORCID identification number(s) for the author(s) of this article can be found under: https://doi.org/10.1002/anie.201800705.

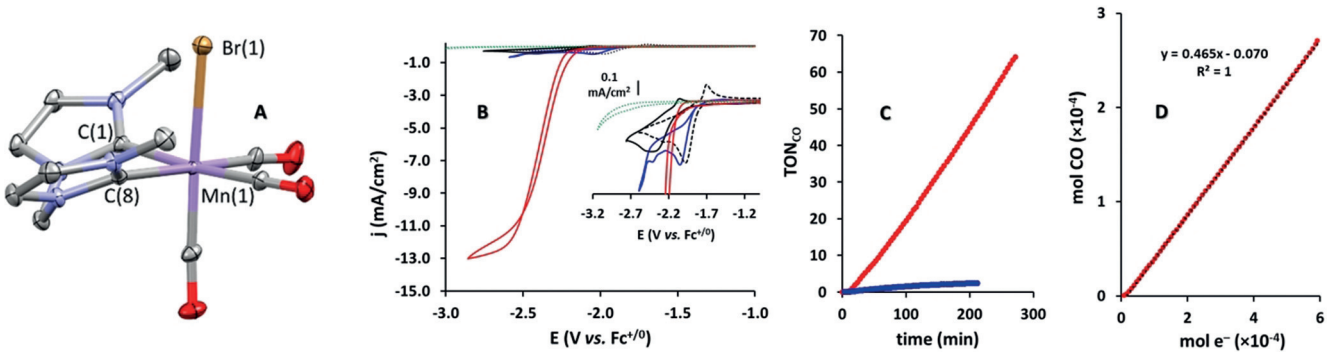

Figure 2. A) X-ray crystal structure of **1**. B–D) Electrochemical behaviour of **1** and **2** (1 mM) in anhydrous 0.1 M $TBAPF_6/CH_3CN$ electrolyte. B) CVs under Ar atmosphere (**1** and **2**: solid and dashed black lines, respectively) and under CO_2-saturated atmosphere (**1**: red; **2**; blue) at $\nu = 0.1\ V s^{-1}$. The green dotted line represents the blank electrolyte under CO_2. C) The amount of CO formed during CPE experiments under CO_2 atmosphere with **1** and **2** at $E_{appl} = -2.32$ V (red) and −2.57 V (blue), respectively. D) Linear correlation between the number of moles of produced CO and the electrons consumed during CPE of **1**.

Cyclic voltammetry (CV) analysis of **1** revealed a main reduction event at $E_p = -2.30$ V (all reduction potentials are reported vs. $Fc^{+/0}$ unless otherwise specified), which is approximately 300 mV cathodically shifted with respect to the corresponding redox wave found for complex **2** ($E_p = -1.97$ V), reflecting the stronger electron-donating properties of the bis-^{Me}NHC ligand. In agreement with FTIR-SEC data (see below) and previous studies,[4,10,11] the observed redox events involve a $2e^-$ reduction of **1** (or **2**) to generate a five-coordinate anion, $[Mn(CO)_3(bis\text{-}^{Me}NHC)]^-$ (**1**$^-$) (or $[Mn(CO)_3(py\text{-}^{Me}NHC)]^-$, **2**$^-$), after loss of the axial Br^- (or I^-). An additional minor feature in the CVs of **1** ($E_p = -2.47$ V) merges with the main wave at high scan rates. CVs at different scan rates indicate reductive diffusion-limited processes for **1** (Figures S8–S10).

Under CO_2 atmosphere, CVs of **1** show a dramatic current increase at the first reduction wave (ca. 35-fold) with an onset potential at approximately −2.12 V and a current plateau at about −2.60 V (Figure 2B). This is in sharp contrast to the behaviour of **2**, which displays only a very small increase in current with a maximum at comparable reduction potentials (−2.56 V; Figures 2B and S9). Furthermore, it is worth noting that there are only a few examples of molecular Mn^I complexes that are able to electrocatalytically activate CO_2 in anhydrous CH_3CN, and those reported have considerably lower activity than **1**.[6a,11]

For complex **1**, the S-shaped catalytic wave, independent of the scan rate, is indicative of a purely kinetic regime for catalytic CO_2 reduction. This behaviour results in a maximum turnover frequency (TOF_{max}) of $2100\ s^{-1}$ under CO_2 atmosphere in neat CH_3CN estimated from CV (see Figures S11 and S12).[12] Notably, the calculated TOF_{max} is more than 2000 times higher than the values reported for analogous pyridyl-NHC catalysts under more favourable conditions (CH_3CN + 5% H_2O),[10a] and about 50 times higher than the highest CO_2 reduction TOF ever reported for an NHC-containing Mn^I catalyst.[10c] Moreover, the TOF_{max} value of **1** is of about the same order of magnitude as the ones calculated for common bpy-based Mn^I complexes (Table S1).[6] The linear increase in the catalytic current with the Mn complex concentration is also consistent with the molecular nature of the catalyst (Figure S13).

Controlled potential electrolysis (CPE) of **1** (1 mM) under a constant CO_2 flow (30 mL min^{-1}) in anhydrous CH_3CN was performed to study its durability and selectivity (Figures S14–S18). On-line gas chromatography (GC-TCD) analysis of the headspace allowed for quantification of the gaseous products. At an applied potential of −2.32 V, an average electrocatalytic current of about 2.5 mA cm^{-2} and linear variation of charge over time were observed throughout the experiment, leading to catalytic CO production with a high faradaic efficiency ($\eta_{CO} \approx 92\%$), without any detectable traces of H_2 (Figures 2C, D). A charge of 50 C passed over 4 h corresponds to a TON_{CO} value of 56, without any substantial decrease in catalytic activity. Electrolysis for extended periods of time revealed prolonged catalyst durability, exceeding turnovers of 100 after 8 h with an excellent selectivity to CO. Catalytically active nanoparticles were discarded by the negligible current observed after a "rinse test" performed after CPE. Remarkably, at a 250 mV more cathodic applied potential ($E_{appl} = -2.57$ V), the reference compound **2** showed a significantly lower electrocatalytic current (ca. 0.5 mA cm^{-2}) than **1** under the same experimental conditions (CO_2 in dry CH_3CN). Moreover, the average faradaic efficiency of **2** was fairly low (after 3.5 h, $\eta_{CO} \approx 22\%$, $TON_{CO} \approx 2.5$; Figures 2C, S19, and S20).

We employed FTIR-SEC to gain insight into the main species involved in the reduction catalysed by **1**. Under Ar atmosphere, when the applied potential matched the reduction wave of **1** (ca. −2.30 V), the bands belonging to **1** ($\nu_{CO} = 2007, 1922, 1887\ cm^{-1}$) started to disappear, giving rise to new CO stretches at 1827, 1731, and 1713 cm^{-1}, which can be assigned to the doubly reduced **1**$^-$ anion.[4d] This assignment is corroborated by the excellent correlation between the experimental and DFT-calculated IR spectra of **1**$^-$. The growth of a broad visible band ($\lambda_{max} = 527$ nm) in a UV/Vis SEC experiment is in agreement with the formation of **1**$^-$ as the main species (Figures S22–S24 and Table S2).[4a,d]

Taken together, these results account for the direct conversion of the initial species, **1**, into five-coordinate **1**$^-$,

which is the predominant product formed upon reduction. Importantly, the low-energy nature of the experimental CO stretches of $\mathbf{1}^-$ indicates a strongly localized negative charge on the Mn atom, which is consistent with the redox innocence of the bis-^{Me}NHC ligand. Indeed, comparison of the Kohn–Sham orbitals of $\mathbf{1}^+$ to those of [Mn(CO)$_3$(bis-^{Me}NHC)]$^{\bullet}$ ($\mathbf{1}^{\bullet}$) and $\mathbf{1}^-$ shows that the reduction takes place exclusively over the metal centre. The HOMO orbital of $\mathbf{1}^-$, unlike that of $\mathbf{2}^-$, is clearly accessible to engage in a nucleophilic attack (Figure S34).

This is reflected by the thermodynamics of the reactions with CO_2, which are exergonic for $\mathbf{1}^-$ but endergonic for $\mathbf{2}^-$ (Scheme 1 and Figures S35–S41). Moreover, the rate-determining step for the catalytic cycle is the C–O cleavage, with an energy barrier as low as 20.1 kcal mol^{-1} for **1** and a higher one for **2** (26.8 kcal mol^{-1}), in good agreement with the catalytic activity.

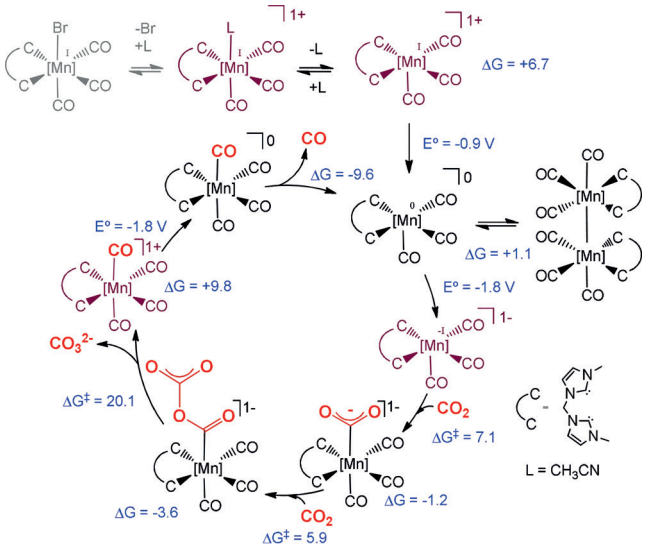

Scheme 1. Proposed mechanism for the reduction of CO_2 to CO by **1**. The energies and redox potentials (vs. SHE) given were determined by DFT calculations at the solvent-corrected B3LYP/6-31+g** level of theory. Mn species experimentally detected by FTIR-SEC are shown in purple.

When a solution of **1** was saturated with CO_2, bands at 1685 and 1646 cm^{-1}, related to free HCO_3^-/CO_3^{2-}, rapidly increased in intensity at the onset potential of the catalytic wave. Sustained CO evolution prevents further monitoring of the reaction. During the reduction, the CO stretches of the initial complex **1** decreased in intensity, with concomitant growth of a new set of low-intensity bands at 2090, 2002, and 1969 cm^{-1}, without any evidence for $\mathbf{1}^-$ formation. Differential IR spectra confirmed the formation of a new species, which was assigned to the tetracarbonyl intermediate [Mn(CO)$_4$(bis-^{Me}NHC)]$^+$ (**1-CO**$^+$), as corroborated also by the theoretical IR spectrum (Figures S23–S26). This is the first direct evidence for this type of intermediate under catalytic conditions. An analogous ν_{CO} pattern has recently been found for a structurally similar complex, which was synthesized under CO atmosphere with a bpy-based Mn^I catalyst.[4e]

The addition of a relatively small amount of water (0.09 M) to a CO_2-saturated solution of **1** significantly boosted the catalytic response, providing a peak-shaped CV with a maximum at −2.61 V (Figure S27). Titration with different aliquots of added water to a CH_3CN solution of **1** highlighted two distinct regimes. At low water concentrations ([H$_2$O] = 0.09–0.56 M), the current tends to increase linearly with [H$_2$O], reaching a maximum activity (>150-fold) for [H$_2$O] = 0.56 M (Figure 3A). At high scan rates (ν > 50 V s^{-1}), plateau-shaped catalytic voltammograms were progressively achieved,[12] leading to a TOF$_{max}$ value of 3.2 × 10^5 s^{-1} for **1** in wet CH_3CN ([H$_2$O] = 0.56 M, Figure 3B). In contrast, the pyridyl-NHC complex **2** displayed only a modest increase in the catalytic current upon increasing the water content in CH_3CN under CO_2 atmosphere, in agreement with previous reports.[10] Nevertheless, a further increase in the water concentration rapidly reduced the catalytic current ([H$_2$O] > 0.56 M, Figure 3A). The inhibiting effect of Brønsted

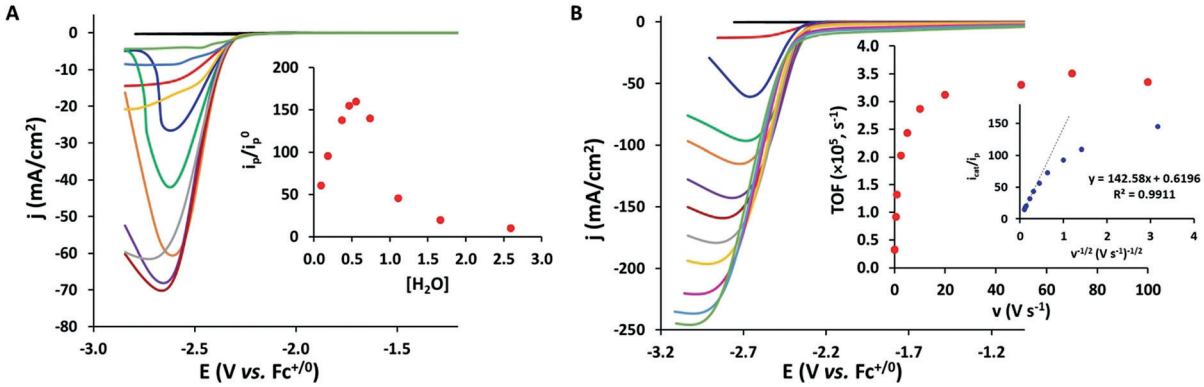

Figure 3. A) Linear scan voltammograms (LSVs) of **1** (1 mM) under CO_2 atmosphere in TBAPF$_6$/CH_3CN (0.1 M) in the presence of [H$_2$O] = 0.09 M (blue), 0.19 M (green), 0.37 M (orange), 0.46 M (violet), 0.56 M (brown), 0.74 M (grey), 1.11 M (yellow), 1.67 M (light blue), and 2.59 M (light green) at ν = 0.1 V s^{-1}. Inset: Peak currents under CO_2 in the presence of various [H$_2$O] (i_p) were normalized to the peak current under Ar (i_p^0). B) LSVs of **1** (1 mM) under CO_2 atmosphere in TBAPF$_6$/CH_3CN (0.1 M) in the presence of 0.56 M H_2O at ν = 0.1 (blue), 0.5 (green), 1 (orange), 2.5 (violet), 5 (brown), 10 (grey), 20 (yellow), 50 (pink), 70 (light blue), or 100 V s^{-1} (light green). Insets: Plot of TOF versus ν (0.1–100 V s^{-1}), highlighting that steady-state conditions are reached at high scan rates (TOF$_{max}$ = 3.2 ± 0.1 × 10^5 s^{-1}). In (A) and (B), CVs of **1** recorded under anhydrous conditions under Ar and CO_2 atmosphere are shown in black and red, respectively.

acids on Mn^I electrocatalysts has recently been highlighted elsewhere.[4e,6a] No electrocatalytic wave was observed with **1** under Ar atmosphere, over a wider range of H_2O/CH_3CN mixtures ($[H_2O] = 0.09–2.60$ M), suggesting selective CO_2 over H^+ reduction (Figure S28). In this regard, CPE ($E_{appl} = -2.32$ V) of **1** (1 mM) in aqueous CH_3CN (0.22 M H_2O) results in quantitative CO production ($\eta_{CO} = 98\%$) for more than 6 h (Figures S31–S33), without formation of H_2. Nevertheless, catalyst deactivation appears to be significantly faster than under anhydrous conditions.

In summary, we have reported the first family of purely organometallic NHC-based tricarbonyl Mn^I complexes that are active in the electrocatalytic reduction of CO_2 to CO. The replacement of a pyridine ring with an NHC unit had a significant effect on the catalytic performance, substantially improving the TOF_{max} and selectivity for CO production of well-established C,N-ligand-based Mn systems. Furthermore, the novel bis-NHC catalyst efficiently and selectively converted CO_2 into CO in anhydrous aprotic organic solvents, whereas the majority of classical bpy-based systems are reported to be inactive without an explicit proton source.[4a–c,e] The estimated TOF_{max} for **1** upon addition of moderate amounts of water is several orders of magnitude higher than those commonly reported for Mn complexes containing functionalized polypyridyl motifs under considerably more acidic conditions.[4a–e] Complementary FTIR-SEC measurements and computational data suggest that the strongly nucleophilic character of the Mn atom is likely responsible for the positive ligand effect on catalysis. We believe that the unique aspects exhibited by this novel family of CO_2 reduction complexes, together with the synthetic viability of ligand modification, open new perspectives for the design of more efficient molecular catalysts.

Acknowledgements

We would like to thank the European Commission (ERC-CG-2014–648304, J.L.-F.). Financial support from the ICIQ Foundation and the CELLEX Foundation through the CELLEX-ICIQ high-throughput experimentation platform and the Starting Career Program is gratefully acknowledged. We also thank the CERCA Programme (Generalitat de Catalunya); MINECO is acknowledged for the ICIQ-IPMP program (F.F.) and Severo Ochoa Excellence Accreditation 2014–2018 (SEV-2013-0319). FCT (Portugal) is acknowledged for projects UID/Multi/04551/2013, RECI/BBB-BQB/0230/2012 (NMR facilities), grant PD/BD/105994/2014 (M.F.P.), and contract IF/00346/2013 (B.R.). We also thank CARISMA, COST Action CM1205 for networking.

Conflict of interest

The authors declare no conflict of interest.

Keywords: carbon dioxide · electrocatalysis · manganese · N-heterocyclic carbenes · spectroelectrochemistry

How to cite: *Angew. Chem. Int. Ed.* **2018**, *57*, 4603–4606
Angew. Chem. **2018**, *130*, 4693–4696

[1] a) J. Qiao, Y. Liu, F. Hong, J. Zhang, *Chem. Soc. Rev.* **2014**, *43*, 631; b) R. Francke, B. Schille, M. Roemelt, *Chem. Rev.* **2018**, https://doi.org/10.1021/acs.chemrev.7b00459.

[2] a) H. Takeda, C. Cometto, O. Ishitani, M. Robert, *ACS Catal.* **2017**, *7*, 70; b) N. Elgrishi, M. B. Chambers, X. Wang, M. Fontecave, *Chem. Soc. Rev.* **2017**, *46*, 761; c) K. A. Grice, *Coord. Chem. Rev.* **2017**, *336*, 78.

[3] a) J. Bonin, A. Maurin, M. Robert, *Coord. Chem. Rev.* **2017**, *334*, 184; b) I. Azcarate, C. Costentin, M. Robert, J.-M. Savéant, *J. Am. Chem. Soc.* **2016**, *138*, 16639.

[4] a) M. Bourrez, F. Molton, S. Chardon-Noblat, A. Deronzier, *Angew. Chem. Int. Ed.* **2011**, *50*, 9903; *Angew. Chem.* **2011**, *123*, 10077; b) J. M. Smieja, M. D. Sampson, K. A. Grice, E. E. Benson, J. D. Froehlich, C. P. Kubiak, *Inorg. Chem.* **2013**, *52*, 2484; c) M. D. Sampson, A. D. Nguyen, K. A. Grice, C. E. Moore, A. L. Rheingold, C. P. Kubiak, *J. Am. Chem. Soc.* **2014**, *136*, 5460; d) F. Franco, C. Cometto, L. Nencini, C. Barolo, F. Sordello, C. Minero, J. Fiedler, M. Robert, R. Gobetto, C. Nervi, *Chem. Eur. J.* **2017**, *23*, 4782; e) K. T. Ngo, M. McKinnon, B. Mahanti, R. Narayanan, D. C. Grills, M. Z. Ertem, J. Rochford, *J. Am. Chem. Soc.* **2017**, *139*, 2604; f) M. D. Sampson, C. P. Kubiak, *J. Am. Chem. Soc.* **2016**, *138*, 1386.

[5] B. Reuillard, K. H. Ly, T. E. Rosser, M. F. Kuehnel, I. Zebger, E. Reisner, *J. Am. Chem. Soc.* **2017**, *139*, 14425.

[6] a) G. K. Rao, W. Pell, I. Korobkov, D. Richeson, *Chem. Commun.* **2016**, *52*, 8010; b) S. J. P. Spall, T. Keane, J. Tory, D. C. Cocker, H. Adams, H. Fowler, A. J. H. M. Meijer, F. Hartl, J. A. Weinstein, *Inorg. Chem.* **2016**, *55*, 12568.

[7] a) Q. Zeng, J. Tory, F. Hartl, *Organometallics* **2014**, *33*, 5002; b) M. V. Vollmer, C. W. Machan, M. L. Clark, W. E. Antholine, J. Agarwal, H. F. Schaefer, C. P. Kubiak, J. R. Walensky, *Organometallics* **2015**, *34*, 3.

[8] a) D. J. Nelson, S. P. Nolan, *Chem. Soc. Rev.* **2013**, *42*, 6723; b) M. N. Hopkinson, C. Richter, M. Schedler, F. Glorius, *Nature* **2014**, *510*, 485; c) E. Peris, *Chem. Rev.* **2018**, https://doi.org/10.1021/acs.chemrev.6b00695; d) C. Johnson, M. Albrecht, *Coord. Chem. Rev.* **2017**, *352*, 1.

[9] a) V. S. Thoi, C. J. Chang, *Chem. Commun.* **2011**, *47*, 6578; b) V. S. Thoi, N. Kornienko, C. G. Margarit, P. Yang, C. J. Chang, *J. Am. Chem. Soc.* **2013**, *135*, 14413; c) M. Sheng, N. Jiang, S. Gustafson, B. You, D. H. Ess, Y. Sun, *Dalton Trans.* **2015**, *44*, 16247; d) J. A. Therrien, M. O. Wolf, B. O. Patrick, *Inorg. Chem.* **2014**, *53*, 12962; e) J. D. Cope, N. P. Liyanage, P. J. Kelley, J. A. Denny, E. J. Valente, C. E. Webster, J. H. Delcamp, T. K. Hollis, *Chem. Commun.* **2017**, *53*, 9442.

[10] a) J. Agarwal, T. W. Shaw, C. J. Stanton, G. F. Majetich, A. B. Bocarsly, H. F. Schaefer III, *Angew. Chem. Int. Ed.* **2014**, *53*, 5152; *Angew. Chem.* **2014**, *126*, 5252; b) J. Agarwal, C. J. Stanton III, T. W. Shaw, J. E. Vandezande, G. F. Majetich, A. B. Bocarsly, H. F. Schaefer III, *Dalton Trans.* **2015**, *44*, 2122; c) C. J. Stanton, J. E. Vandezande, G. F. Majetich, H. F. Schaefer, J. Agarwal, *Inorg. Chem.* **2016**, *55*, 9509.

[11] F. Franco, C. Cometto, F. F. Vallana, F. Sordello, E. Priola, C. Minero, C. Nervi, R. Gobetto, *Chem. Commun.* **2014**, *50*, 14670.

[12] a) C. Costentin, S. Drouet, M. Robert, J.-M. Savéant, *J. Am. Chem. Soc.* **2012**, *134*, 11235; b) C. Costentin, M. Robert, J.-M. Saveant, *Chem. Soc. Rev.* **2013**, *42*, 2423; c) C. Costentin, J.-M. Savéant, *ChemElectroChem* **2014**, *1*, 1226.

Manuscript received: January 20, 2018
Accepted manuscript online: February 26, 2018
Version of record online: March 14, 2018

